Published for SISSA by Springer

Received: February 25, 2014
Revised: September 26, 2014
Accepted: October 2, 2014
Published: October 30, 2014

Higgs boson CP-properties of the gluonic contributions in Higgs plus three jet production via gluon fusion at the LHC

Francisco Campanario[a,b] **and Michael Kubocz**[c,b]

[a] *Theory Division, IFIC, University of Valencia-CSIC, E-46100 Paterna, Valencia, Spain*

[b] *Institute for Theoretical Physics, KIT, 76128 Karlsruhe, Germany*

[c] *Institut für Theoretische Teilchenphysik und Kosmologie, RWTH Aachen University, D52056 Aachen, Germany*

E-mail: francisco.campanario@ific.uv.es, kubocz@physik.rwth-aachen.de

Abstract: In high energy hadronic collisions, a general CP-violating Higgs boson Φ with accompanying jets can be efficiently produced via gluon fusion, which is mediated by heavy quark loops. In this article, we study the dominant sub-channel $gg \to ggg\Phi$ of the gluon fusion production process with triple real emission corrections at order α_s^5. We go beyond the heavy top-quark approximation and include the full mass dependence of the top- and bottom-quark contributions. Furthermore, in a specific model we demonstrate the features of our program and show the impact of bottom-quark loop contributions in combination with large values of $\tan\beta$ on differential distributions sensitive to CP-measurements of the Higgs boson.

Keywords: QCD Phenomenology, Monte Carlo Simulations

ArXiv ePrint: 1402.1154

doi:10.1007/JHEP10(2014)173

JHEP10(2014)173

Contents

1 Introduction

Since the discovery of a new bosonic resonance within a mass range of 125–126 GeV at the Large Hadron Collider (LHC) [1, 2], the measurement of its properties with the aim to validate the Standard Model (SM) Higgs boson hypothesis has become one of the main goals of the scientific community [3–19]. Recent measurements by the ATLAS and the CMS collaborations favor a spin-0 Higgs boson with positive parity [20–26], while a pure *CP*-odd scalar Higgs particle was discarded in previous studies [14] with more than three standard deviations. However, a *CP*-violating scalar Higgs boson, Φ, formed by a mixture of a *CP*-even SM-like scalar, H, and a *CP*-odd scalar A as follows,

$$\Phi = H\cos\alpha + A\sin\alpha\,, \tag{1.1}$$

where α is the corresponding mixing angle, has not yet been ruled out. It is known that Higgs production in association with two jets via gluon fusion (GF) is a promising channel in order to measure the *CP*-properties of the Higgs particle as well as its coupling to fermions [27, 28]. The production of $\Phi + 2$ jet events leads to a distinctively altered distribution of the azimuthal angle difference between the two jets. The minima of the distribution are found at $\phi_{jj}^{\min} = \pm\pi/2$ for a pure *CP*-even Higgs (i.e. $\Phi = H$), or at $\phi_{jj}^{\min} = 0, \pm\pi$ for a pure *CP*-odd Higgs (i.e. $\Phi = A$) [4, 29–32]. For a *CP*-violating mixed Higgs boson state, the location of the minima shifts. Thus, the azimuthal angle distribution of Φjj production provides valuable information about the mixing of the scalar particle.

A relevant aspect of interest is the modification of these azimuthal angle correlations by the emission of additional jets, that is, at least by a third jet. Several analyses [33–35] demonstrated that the ϕ_{jj}-correlations survive with minimal modifications if the hard radiation is separated from the parton shower and the hadronization effects. Similar conclusions were obtained by a parton level calculation of the GF induced Higgs plus two jet production process at NLO [36, 37] within the framework of the heavy top-quark effective theory.

JHEP10(2014)173

For a Higgs mass lower than the top-quark mass, the total cross section can be determined with good accuracy using the effective Lagrangian approach, derived from the heavy top-quark approximation. The range of validity of the effective approach has been studied at LO for Φjj production in ref. [32], and recently for $Hjjj$ production in ref. [38], for which also NLO corrections are available within the effective theory approach [39].

When the Higgs/jet transverse momentum and/or the Higgs mass become larger than the top-quark mass, as also when bottom-quark induced loop contributions receive a strong enhancement (for example, in two Higgs doublet models (2HDM), like the Minimal Supersymmetric Standard Model (MSSM), due to the large ratio of the two vacuum expectation values, $v_u/v_d = \tan\beta$ (see eq. (2.8))), the effective Lagrangian approximation breaks down and leads to unreliable predictions. In these regions therefore it becomes necessary to switch to the full theory and take the full quark mass dependence into account.

In this article, we present LO results for the sub-process $gg \to ggg\Phi$, which is the dominant channel of the Φ + three jet production process, and hence, an essential piece to compute the real emission contributions for Higgs plus two jet production at NLO via gluon fusion within the full theory. Including the full mass dependence of the top- and bottom-quark contributions, we analyze whether the azimuthal angle correlations survive in the presence of additional radiation. The calculation involves massive rank-5 hexagon Feynman diagrams, which are the most complicated topologies appearing in Higgs production in association with three jets via GF, hence providing an essential basis to check the numerical stability of the full process. This is particularly important for the numerically challenging bottom-quark loop corrections, which turn out to provide the main contribution at large values of $\tan\beta$. Results for the full process and a detailed description of de-correlation effects will be given in a forthcoming publication.

This article is organized as follows. Some basic theoretical ingredients are given in section 2. The technical details of our implementation are presented in section 3. Numerical results are shown in section 4 and, finally, we conclude in section 5.

2 Theoretical setup

The *CP*-properties of the Higgs particle can be studied starting with the Lagrangian,

$$\mathcal{L}_{\text{Yukawa}} = y_q\, \bar{q}\, q\, H + \mathrm{i}\tilde{y}_q \bar{q}\gamma_5\, q\, A\,, \tag{2.1}$$

with H and A representing a *CP*-even and a *CP*-odd Higgs boson respectively, and y_q and $\tilde{y}_q$ their Yukawa couplings to fermions q. A scalar *CP*-violating Higgs boson Φ, formed by a mixing of a *CP*-odd and a *CP*-even Higgs states is described by

$$\begin{pmatrix} \Phi \\ \Phi' \end{pmatrix} = \begin{pmatrix} \cos\alpha & \sin\alpha \\ -\sin\alpha & \cos\alpha \end{pmatrix} \times \begin{pmatrix} H \\ A \end{pmatrix}, \tag{2.2}$$

where α denotes the mixing angle and Φ', an orthogonal state, which we will assume to be much heavier than Φ and therefore strongly suppressed in possible production processes.

JHEP10(2014)173

Thus, inverting the matrix of eq. (2.2), replacing the *CP*-eigenstate fields in terms of the mixed ones in eq. (2.1), and omitting the Φ' field, the Lagrangian reads

$$\mathcal{L}_{\text{Yukawa}} = \overline{q}\,(Y_q + \mathrm{i}\gamma_5 \tilde{Y}_q)\, q\, \Phi\,. \tag{2.3}$$

Here Y_q and $\tilde{Y}_q$ represent general Yukawa couplings which are functions of the mixing angle α, i.e., $Y_q = y_q \cos\alpha$ and $\tilde{Y}_q = \tilde{y}_q \sin\alpha$. Hence, for $\alpha = 0$ and $\alpha = \pi/2$, we recover the purely *CP*-even and *CP*-odd Higgs states respectively.

In the SM, Higgs production modes with bottom-quark loop contributions are usually neglected, as they suffer a strong suppression due to the smallness of the Yukawa coupling $y_b^{\text{SM}} = m_b/v$, resulting from the small bottom-quark mass m_b (here $v = 246\,\text{GeV}$ denotes the SM vacuum expectation value). The remaining top-quark loop effects can be reduced to a simplified form within the heavy top-quark mass limit [40, 41], so that the effective Lagrangian, including a *CP*-odd Higgs component, is given by

$$\mathcal{L}_{\text{eff}} = y_t \cdot \frac{\alpha_s}{12\pi m_t} \cdot H\, G^a_{\mu\nu}\, G^{a\,\mu\nu} + \tilde{y}_t \cdot \frac{\alpha_s}{8\pi m_t} \cdot A\, G^a_{\mu\nu}\, \tilde{G}^{a\,\mu\nu}, \tag{2.4}$$

where $G^a_{\mu\nu}$ represents the gluon field strength and $\tilde{G}^{a\,\mu\nu} = 1/2\, G^a_{\rho\sigma}\, \varepsilon^{\mu\nu\rho\sigma}$ its dual. Accordingly, the Lagrangian for a general *CP*-violating Higgs can be written by

$$\mathcal{L}_{\text{eff}} = \left(Y_t \cdot \frac{\alpha_s}{12\pi m_t}\, G^a_{\mu\nu}\, G^{a\,\mu\nu} + \tilde{Y}_t \cdot \frac{\alpha_s}{8\pi m_t}\, G^a_{\mu\nu}\, \tilde{G}^{a\,\mu\nu} \right) \Phi\,. \tag{2.5}$$

Note that the top-quark mass drops out if quark mass dependent Yukawa couplings are taken into account. Often, the predictions obtained by the effective theory approximation already include form factors (FF), which re-scale the corresponding Yukawa couplings thereby reintroducing missing quark mass dependencies. The form factors are derived from the partial decay width of the Higgs boson to two gluons and are therefore proportional to triangle fermion-loops. Their *CP*-odd and *CP*-even components are given by [7, 42]

$$\begin{aligned} \text{FF}_A(\tau) &= 2\,\tau^{-1} f(\tau)\,, \\ \text{FF}_H(\tau) &= 2\left(\tau + (\tau - 1) f(\tau)\right)\tau^{-2}, \end{aligned} \tag{2.6}$$

with the universal scaling function

$$f(\tau) = \begin{cases} \arcsin^2 \sqrt{\tau} & \tau \leq 1 \\ -\frac{1}{4}\left[\log \frac{1+\sqrt{1-\tau^{-1}}}{1-\sqrt{1-\tau^{-1}}} - \mathrm{i}\pi \right]^2 & \tau > 1\,, \end{cases} \tag{2.7}$$

and scaling variable $\tau = m_\Phi^2/4m_i^2$. Here m_i with $i = t, b$ denotes the corresponding loop mass and m_Φ the Higgs boson mass.[1] As discussed previously, the validity of the effective theory approximation within the SM restricts the Higgs masses and values of the transverse momentum of the jets to be lower than the top-quark mass. Furthermore, in contrast to SM, in a 2HDM the Yukawa coupling of a down-type quark is not necessarily suppressed

[1] For the calculation of the form factors, MadGraph4 uses the Taylor-expanded version for $\tau \leq 1$.

JHEP10(2014)173

compared to that of the corresponding up-type quark. For example, in the Type II model, the up- and down-type Yukawa couplings for the *CP*-odd components are given by,

$$\tilde{y}_u^{\rm II} = -\frac{\cot\beta}{v} m_u \qquad \text{and} \qquad \tilde{y}_d^{\rm II} = -\frac{\tan\beta}{v} m_d\,, \tag{2.8}$$

where the SM-like vacuum expectation value $v = \sqrt{v_d^2 + v_u^2} = 246\,\text{GeV}$ and $\tan\beta = v_u/v_d$ are functions of two vacuum expectation values. This implies that for large values of $\tan\beta$, the down-type quarks Yukawa coupling is enhanced, while the Yukawa coupling of up-type quarks is suppressed by $\cot\beta$. Due to this enhancement, loops with bottom-quarks can also provide significant contributions to the total cross section as well as to differential distributions of important observables, rendering the predictions of the effective theory unreliable. Henceforth, we will include bottom-quark loop corrections in our study to investigate their phenomenological effects beyond the validity bounds of the effective theory approximation (with and without form factors) and the numerical behavior of our program for Φjjj production.

3 Calculational details

The subprocesses relevant to Φjjj production are,

$$\begin{aligned} q\,q &\to q\,q\,g\,\Phi\,, \qquad q\,Q \to q\,Q\,g\,\Phi\,, \\ q\,g &\to q\,g\,g\,\Phi\,, \qquad g\,g \to g\,g\,g\,\Phi\,, \end{aligned} \tag{3.1}$$

together with the corresponding cross-related processes, which we have not shown explicitly. We restrict our study to the last sub-process, which, we reiterate, contains the most complicated topologies that appear in any Higgs production process in association with three jets via GF. This is also the subprocess that is enhanced by the large gluon flux at the LHC. To perform the numerical analysis, we closely follow the setup of $Hjjj$ production, described in ref. [38], and use our implementation (GGFLO MC program), which is a part of the VBFNLO framework [43–45]. As is customary in VBFNLO calculations, we use the effective current approach [46, 47] to evaluate the loop amplitudes. Eight master Feynman diagrams involving four *CP*-even and four *CP*-odd Higgs couplings to fermions are computed for this purpose. Due to the absence of UV-poles, a renormalization procedure was unnecessary, and the calculation was done within the four dimensional Minkowksi space using the anti-commuting prescription of γ_5 [48]. The four *CP*-even/odd Higgs master integrals depicted in figure 1 have been computed within the in-house framework described in ref. [49] — the attached gluons are considered to be off-shell vector currents, which allow the addition of further participating gluons. The numerical evaluation of the tensor integrals follows the Passarino-Veltman approach of ref. [50] up to box-diagrams, while for pentagons and hexagons ref. [51], together with the scheme laid out in ref. [49], is followed. Scalar integrals are computed following refs. [52, 53]. Furthermore, the number of diagrams to be evaluated are reduced by a factor two applying Furry's theorem. The color factors are the same as those for $Hjjj$ production, and were computed by hand and cross-checked with MadGraph4 [54, 55].

JHEP10(2014)173

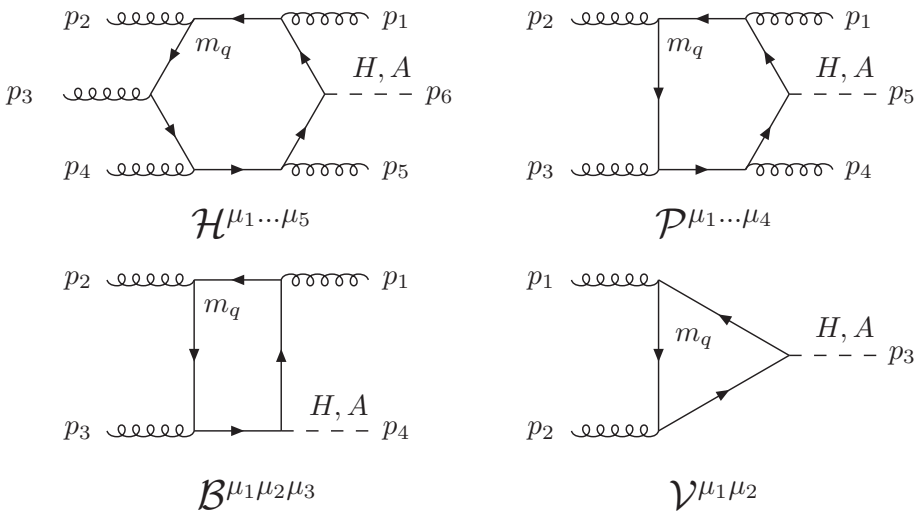

Figure 1. Master Feynman diagrams.

To ensure that our results are correct, we first compare the amplitudes of the *CP*-odd and *CP*-even production modes obtained by MadGraph4 against our own implementation of the Φjjj production channel approximated at the limit of infinite top-quark mass. This implementation is also a part of our GGFLO program. We ensured that for both the *CP*-odd and *CP*-even production modes the agreement of the two results are at the machine precision level and at per mille level when compared at the amplitude level and at the integrated cross section level, respectively. Next we compare the full and effective theory results at the amplitude and integrated cross section levels for $m_t = 5 \cdot 10^4$ GeV within the VBFNLO framework. The agreement is better than one per ten thousand level.

To control the numerical instabilities inherent to a multi-leg calculation, we follow the procedure described in ref. [38]. At this point, we find it relevant to summarize the essential points of this procedure for the sake of clarity. We use the technique of the Ward identities, developed in ref. [49] and applied successfully in other complex GF processes [38, 56]. These identities allow one to relate an N-point tensor integral to an $N-1$-point one by replacing an effective current with the corresponding momentum flow. As this property is transferred to the Master integrals, it provides a strong check of the correctness of these Master integrals. For example, using the Ward identity, a hexagon topology of a rank five tensor can be written as a difference of two pentagon diagrams of rank four tensor

$$\mathcal{H}^{\mu_1\cdots\mu_5} p_{i,\mu_i} = \mathcal{P}_1^{\mu_1\cdots\hat{\mu}_i\cdots\mu_5} - \mathcal{P}_2^{\mu_1\cdots\hat{\mu}_i\cdots\mu_5}, \qquad i = 1\ldots 5\,, \tag{3.2}$$

where $\hat{\mu}_i$ denotes the vertex replaced by the corresponding momentum p_i. We construct all possible Ward identities for each physical permutation of each and every diagram, e.g. all five different possibilities for the hexagon $\mathcal{H}^{\mu_1\cdots\mu_5}$.

For each phase space point of each and every diagram, these Ward identities are evaluated with a small additional computing effort using a cache system. We demand a global accuracy of $\epsilon = 5 \times 10^{-4}$, and if the Ward Identities are still not satisfied, we re-evaluate the diagram using quadruple precision. If at this precision level also the Ward identities

JHEP10(2014)173

are not satisfied, we set the amplitude to zero and discard the phase-space point. The amount of phase-space points which do not pass the Ward identity check after this last step is statistically negligible and well below the per mille level.

Concerning the running time of our MC program, we obtain a statistical error of 1% in 3 hours (top-quark contributions only) for the LO inclusive cross section using a single core of an Intel $i7$-3970X processor with the Intel-ifort compiler (version 12.1.0). The distributions shown below are based on multiprocessor runs with a total statistical error of up to 0.02%. Given the computing time, the precision of our results sets a benchmark for comparisons with automated multi-leg calculation programs.

4 Numerical results

In this section, we present results for integrated cross sections and selected differential distributions of important observables for the sub-process $gg \to ggg\Phi$ at the LHC at 13 TeV center of mass (c.m.) energy. We use the CTEQ6L1 parton distribution functions (PDFs) [57] with the default strong coupling $\alpha_s(M_Z)$ set at 0.130 and the k_T-jet algorithm. To avoid soft and collinear QCD singularities, we introduce a minimal set of cuts for the jets. These jets are ordered in terms of decreasing transverse momenta, $p_T^{j_1} > p_T^{j_2} > p_T^{j_3}$, and the corresponding cuts are given by

$$p_T^{j_n} > 20\,\text{GeV}, \qquad |\eta_{j_n}| < 4.5\,, \qquad R_{j_n j_m} > 0.6\,, \qquad n \neq m = 1,2,3\,, \tag{4.1}$$

where $R_{j_n j_m}$ describes the separation of the two partons in the plane of pseudo-rapidity versus azimuthal-angle,

$$R_{j_n j_m} = \sqrt{\Delta\eta_{j_n j_m}^2 + \varphi_{j_n j_m}^2}\,, \tag{4.2}$$

with $\Delta\eta_{j_n j_m} = |\eta_{j_n} - \eta_{j_m}|$ and $\varphi_{j_n j_m} = \varphi_{j_n} - \varphi_{j_m}$. These cuts anticipate LHC detector capabilities and jet finding algorithms and will be called "inclusive cuts" (IC) in the following.

All quarks, except the bottom- and the top-quark are considered massless. The top-quark mass is fixed at $m_t = 173.3\,\text{GeV}$ and the $\overline{\text{MS}}$ bottom-quark mass at $\overline{m}_b(m_b) = 4.2\,\text{GeV}$. In our setup, the Yukawa couplings contain a 33–51% smaller m_b than the pole mass of 4.855 GeV utilized in the loop propagators within the range of 100–1000 GeV for the Higgs-mass. Although we present an LO calculation, we have taken into account the evolution of m_b up to a reference scale (in this case m_Φ) due to the dominance of the bottom-quark loop contributions at large values of $\tan\beta$. We achieved this using the relation between the pole mass and the $\overline{\text{MS}}$ mass, following refs. [42, 58] within a 5-flavor scheme. The Higgs boson is produced on-shell and without finite width effects. Additionally, we choose $M_Z = 91.188\,\text{GeV}$, $M_W = 80.386\,\text{GeV}$ and $G_F = 1.16637 \times 10^{-5}\,\text{GeV}^{-2}$ as electroweak input parameters and use Standard Model tree level relations to compute the weak mixing angle and the electromagnetic coupling constant.

The factorization scale is set to $\mu_F = (p_T^{j_1} p_T^{j_2} p_T^{j_3})^{1/3}$ and the renormalization to

$$\alpha_s^5(\mu_R) = \alpha_s(p_T^{j_1})\alpha_s(p_T^{j_2})\alpha_s(p_T^{j_3})\alpha_s(p_\Phi)^2. \tag{4.3}$$

JHEP10(2014)173

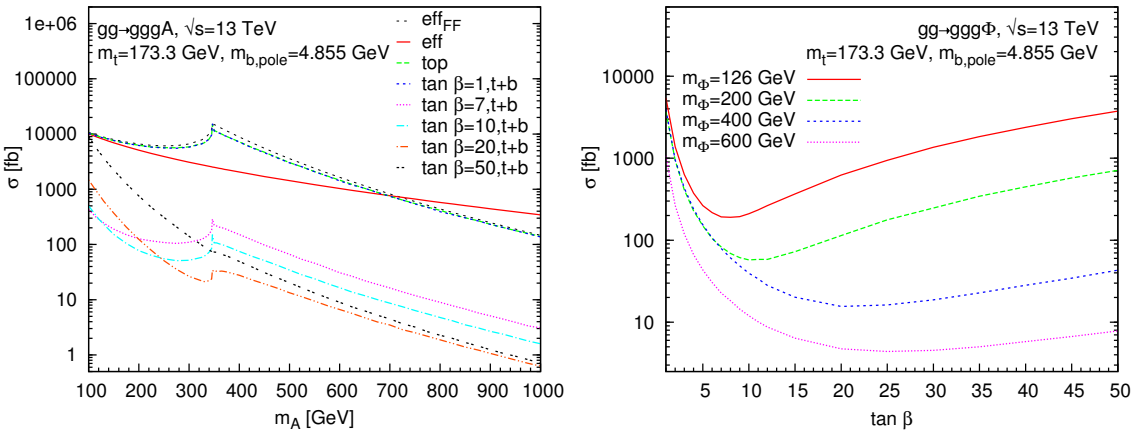

Figure 2. Left: $A + 3$ jet cross section as a function of the pseudo-scalar Higgs boson mass m_A, for different values of $\tan\beta$. Right: $\Phi + 3$ jet cross section as a function of $\tan\beta$ for several values of m_Φ. The inclusive cuts (IC) of eq. (4.1) are applied.

To simulate effects of a general *CP*-violating Higgs boson, we consider a scenario where the Yukawa couplings of the *CP*-even and the *CP*-odd components are of the same strength and equal to the *CP*-odd couplings of the 2HDM of type II, i.e.,

$$y_q = \tilde{y}_q = \tilde{y}_q^{\mathrm{II}}. \tag{4.4}$$

This ensures the same $\tan\beta$ dependence of both couplings. Additionally, unless otherwise stated, we use a mixing angle defined by $\tan\alpha = 2/3$. This choice sets the *CP*-odd and *CP*-even components to equal strength, thereby compensating the enhancement factor of 3/2 of the effective *Agg* coupling due to loop effects (see Lagrangian of eq. (2.4)).

In the left panel of figure 2, the total cross section of a pure *CP*-odd Higgs boson ($\alpha = \pi/2$) is plotted as a function of its mass for different values of $\tan\beta$. One can observe that amplitudes containing both top- and bottom-quark loop corrections, denoted by "t+b" in the following, are indistinguishable from the pure top-quark loop contributions for $\tan\beta = 1$. Both of them show the expected threshold enhancement at a Higgs mass corresponding to twice mass of the top-quark. For configurations dominated by bottom-quark loops, the characteristic peak appears well below the range of the Higgs mass shown in the plots. We also show results for the effective theory approximation with and without corrections to the couplings by the additional form factors (FF) defined in eq. (2.6).

Within a 10% deviation with respect to the full theory, the effective theory gives accurate predictions up to a Higgs mass of 150 GeV. With the inclusion of form factor FF, the range of validity is extended up to about 300 GeV, again within a 10% deviation. Additionally, it brings back the threshold behavior at $m_A = 2\,m_t$. Beyond the validity bound, the total cross section is overestimated up to 20% at $m_A = 370$ GeV followed by a slow convergence to the results of the full theory. Although the form factor predicts the normalization of the cross section for $\tan\beta = 1$ relatively well, large deviations can still be observed in differential distributions even for small Higgs masses, see e.g, ref. [38] and figures 3–4.

JHEP10(2014)173

In the right panel of figure 2, we show the total cross section for Φjjj production as a function of $\tan\beta$ computed within our scenario for different values of Higgs mass. Similar to the Φjj production process [32], in this case the minimum of the cross section for small Higgs masses is obtained near $\tan\beta \approx 7$, when $\tilde{y}_t^{\rm II} \approx \tilde{y}_b^{\rm II}$ (see eq. (2.8)) and both Yukawa couplings are suppressed simultaneously in comparison to $y_t^{\rm SM} = m_t/v$. The shift of the minimum of σ towards larger $\tan\beta$ with increase in m_Φ can be understood in the following way: for large values of $\tan\beta$, e.g. $\tan\beta = 50$ illustrated in the left panel of figure 2, the bottom-quark loop contributions dominate over the top-quark contributions (the latter being suppressed). However, the total cross section decreases rapidly as m_Φ increases, since the mass scale in the loops is now set by the Higgs (being heavier) instead of the (relatively) lighter quark. The bottom-quark loop contributions, at large m_Φ, decrease at a faster rate compared to that of the top-quark loop corrections (curve for $\tan\beta = 50$ vs. that for $\tan\beta = 1$ respectively). This implies that higher values of $\tan\beta$ are needed to effectively set both top- and bottom-quark Yukawa couplings to equal strength. Consequently, the minimum of the distribution shifts towards larger values of $\tan\beta$.[2]

In the following, we simulate effects of a general *CP*-violating Higgs sector at the LHC using the previously described model, keeping the Higgs mass fixed at 126 GeV for a set of different $\tan\beta$ values, and show differential distributions for several observables. Figure 3 shows the transverse momentum distribution of the hardest jet. For large values of $\tan\beta$, the bottom-quark loop corrections have a strong dominance and modify the spectrum. For $p_{T,j} > m_b$ however, the large scale of the kinematic invariants leads to an additional suppression of bottom-quark loop induced sub-amplitudes, compared to that obtained from the effective theory with a heavy top-quark. This is clearly visible, for example, for $\tan\beta = 10$ at 400 GeV in the lower panel of figure 3. Here Kfact, defined as the ratio of the result obtained from the effective theory with a heavy top-quark and that from the full theory at LO, shows a 4-times overestimated result predicted by the effective theory approach. For $\tan\beta = 1$, the effective theory approximation corroborates the full theory prediction within 10% accuracy up to $p_T^{j\max} < 200$ GeV. Beyond this predictions, the two theories start to grow apart, and deviations as high as up to 100% can be found. This observation signifies the limitation of the heavy top-quark approximation used in the effective theory approach, and indicates possible sources of inaccuracy in the results obtained within this approach in scenarios beyond SM. Similar conclusions can also be drawn from figure 4. Here the left panel illustrates the differential distribution of the transverse momentum of the Higgs boson, while the right panel shows the transverse scalar sum of the system defined as $h_{T^*} = \sum_i p_T^{j_i} + \sqrt{p_{T,\Phi}^2 + m_\Phi^2}$. The concept of transverse scalar sum has frequently been advocated in the literature in the context of new physics searches.

The azimuthal angle distribution, defined as the difference of the azimuthal angle between the more-forward and the more-backward of the two tagging jets ($\phi_{j_1 j_2} = \varphi_F - \varphi_B$), is known to be sensitive to the *CP*-nature of the Higgs boson [29]. In ref. [32] it was shown for Φjj production, that the softening effects, observed in the transverse momentum

[2] Qualitatively, this can be understood by plotting $f(\tan\beta) = (\tilde{y}_b^{\rm II})^2 + (\tilde{y}_t^{\rm II})^2 \propto m_b^2 \tan^2\beta + m_t^2 \cot^2\beta$ and effectively reducing the value of m_b to simulate the faster decrease of the bottom-quark loops with increasing Higgs mass.

JHEP10(2014)173

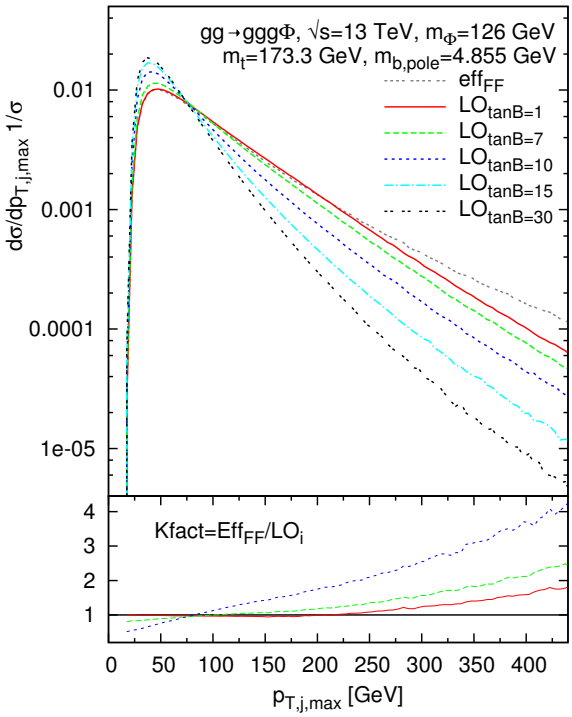

Figure 3. Transverse-momentum distributions of the hardest jet including top- and bottom-quark loop induced amplitudes for different values of $\tan\beta$ and for the effective theory with form factors (eff_{FF}). The lower panel shows the ratios of the effective Lagrangian approach vs. the full theory for different values of $\tan\beta$. The inclusive cuts (IC) of eq. (4.1) and the model of eq. (4.4) with $\tan\alpha = 2/3$ are used.

distributions due to bottom-quark loop corrections, do not modify the jet azimuthal angle correlations predicted by the effective theory approximation. In our case however, the presence of an additional (i.e. third) jet automatically raises the question, as to whether or not this additional radiation distorts these predictions. To address this question, we modify the inclusive set of cuts in order to increase the sensitivity of $\phi_{j_1 j_2}$ distribution to the CP-structure of the Higgs couplings as follows,

$$p_T^{j_n} > 30\,\text{GeV}, \qquad |\eta_{j_n}| < 4.5\,, \qquad R_{j_n j_m} > 0.6\,, \qquad \Delta\eta_{j_1 j_2} > 3\,, \qquad n \neq m = 1,2,3\,. \tag{4.5}$$

The effective theory approach shows a phase shift of the $\phi_{j_1 j_2}$ distribution by an angle $\Delta\phi_{j_1 j_2}$ which is given by the relative strength of the CP-even and CP-odd couplings. Taking into account the relative enhancement of the pure CP-odd coupling due to loop effects (see eq. (2.4)), the phase shift is given by [29],

$$\tan\Delta\phi_{j_1 j_2} = -\frac{3}{2}\frac{\tilde{Y}_q}{Y_q} = -\frac{3}{2}\frac{\tilde{y}_q}{y_q}\tan\alpha\,. \tag{4.6}$$

As mentioned earlier, in our model, we assume $\tan\alpha = 2/3$ and $y_q = \tilde{y}_q = \tilde{y}_q^{\text{II}}$ (see eq. (4.4)). Hence, $(3\tilde{Y}_q)/(2Y_q) = 1$, and the minima are shifted to $\phi_{j_1 j_2}^{\text{min}} = -45°, 135°$

JHEP10(2014)173

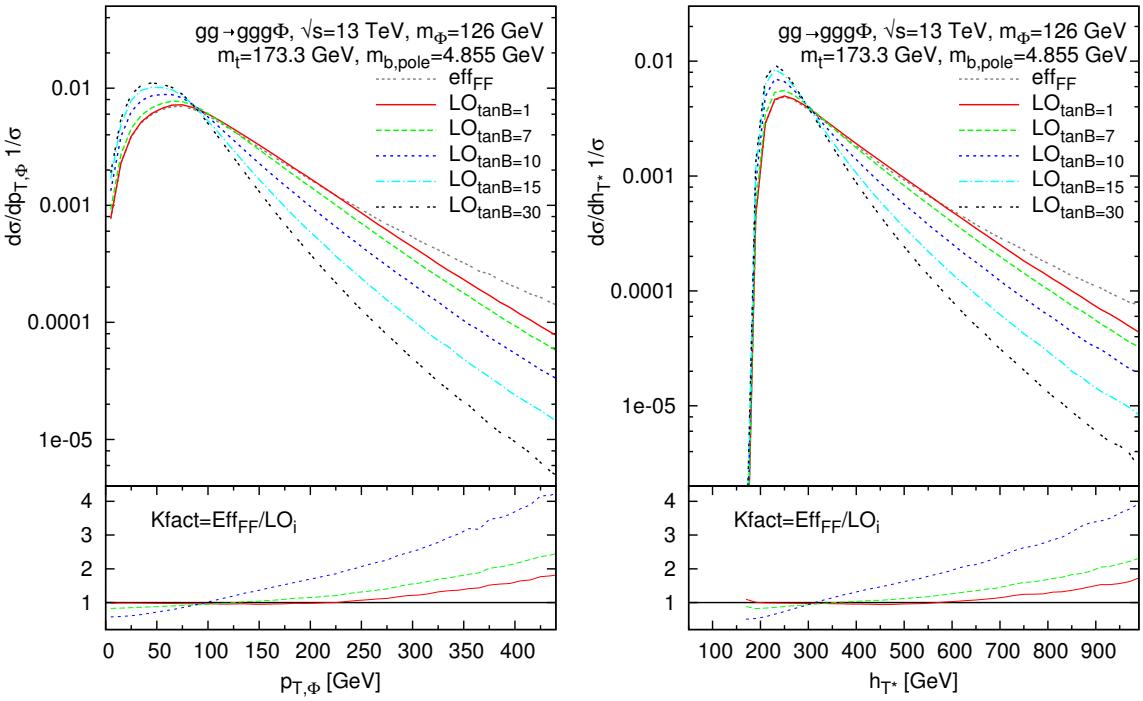

Figure 4. The transverse-momentum distributions of the Higgs boson Φ (left panel) and the transverse scalar sum (right panel), are plotted. Details are described in figure 3 and in the text.

degrees.[3] This can be seen in the left panel of figure 5 where normalized $\phi_{j_1 j_2}$-distributions are plotted. It is clearly visible that the presence of additional radiation does not alter the main characteristics of the azimuthal angle correlations. Additionally, one observes that the effective theory approximation accurately reproduces the shape of the $\phi_{j_1 j_2}$ distribution. In the full theory, the azimuthal angle distributions receive kinematic distortions caused by kinematical effects. These effects are caused by, (1) the balance of the transverse momenta of the jets with respect to that of the Higgs boson due to momentum conservation, and (2) the softer momentum spectrum of the jets and the Higgs boson for high values of $\tan\beta$ (figure 3 and 4) where bottom-quark loop contributions dominate. These features have also been observed in Φjj production in ref. [32].

Finally, in the right panel of figure 5, we show the normalized centralized pseudo-rapidity distribution of the third jet with respect to the tagging jets, $z^* = \big(\eta_{j_3} - 1/2(\eta_{j_1} + \eta_{j_2})\big)/|\eta_{j_1} - \eta_{j_2}|$. For this, in addition to the inclusive cuts of eq. (4.1), we have imposed typical vector fusion cuts

$$m_{j_1 j_2} > 600\,\text{GeV}, \qquad |\eta_{j_1} - \eta_{j_2}| > 4\,, \qquad \eta_{j_1} \cdot \eta_{j_2} < 0\,. \tag{4.7}$$

The variable z^* shows the nature of VBF processes involving the fusion of electro-weak Gauge bosons. In EW $Hjjj$ production [59], one can clearly observe how the third jet

[3] Note that the same shift in $\phi_{j_1 j_2}$ can also be achieved by choosing different values of the mixing angle α and the Yukawa couplings. Instead of requiring equal strength for the Yukawa couplings and $\tan\alpha = 2/3$, in ref. [32] for example, $y_q = 3/2\tilde{y}_q$ and equal strength of the CP-odd and CP-even mixing components with $\alpha = \pi/4$ was used. The normalization of the cross section changes for each choice.

JHEP10(2014)173

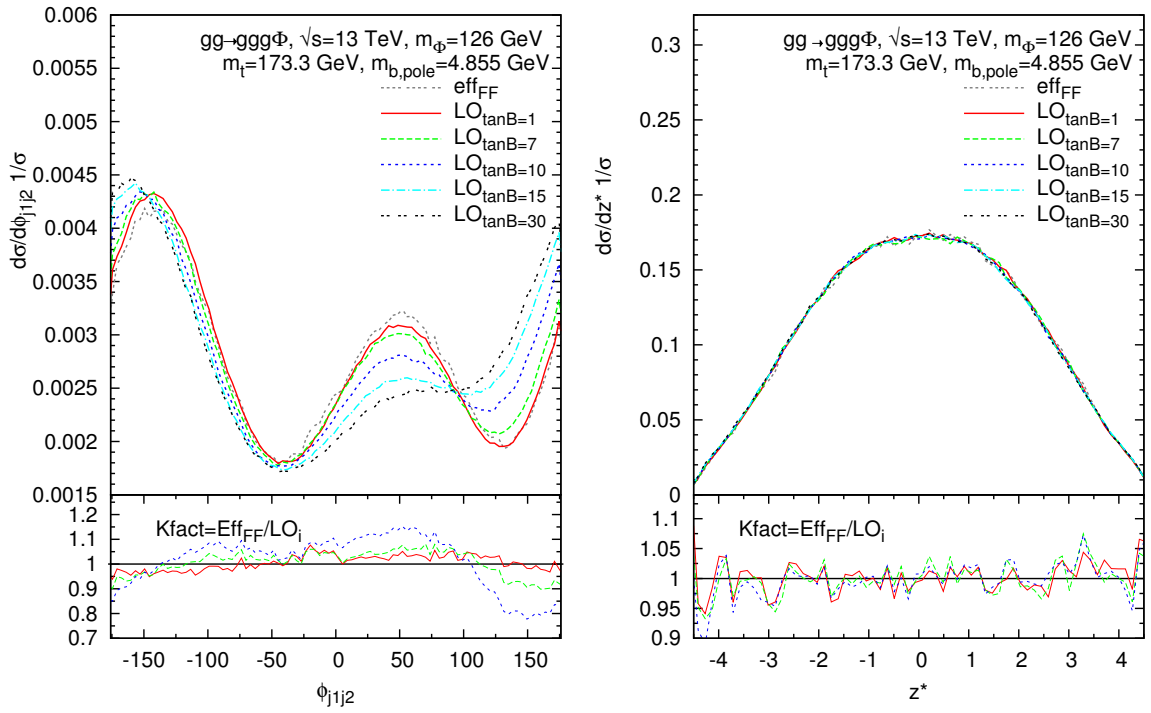

Figure 5. Left: azimuthal angle correlation $\phi_{j_1 j_2}$ of the two hardest jets applying the cuts of eq. (4.5). Right: z^*, the normalized centralized pseudo-rapidity distribution of the third jet w.r.t. the tagging jets using the VBF cuts of eq. (4.7). Further, details are described in figure 3 and in the text.

tends to accompany one of the two leading jets appearing at $1/2$ and $-1/2$ respectively. Additionally, because the EW gauge bosons are colorless, there is almost no jet activity between the two leading tagging-jets in the pseudo-rapidity-gap region (minimum at $z^* = 0$). However, as expected, in our case the typical behavior of a QCD induced process is observed, and the pseudo-rapidity gap between the two jets is filled up by at least a third jet due to additional gluon radiation. Furthermore, the shape of the z^*-distribution is insensitive to the change of the Higgs couplings to fermions brought about by the model parameter $\tan\beta$. Further *CP*-measurement studies beyond our model, the results for the full process, and a detailed description of de-correlation effects are to appear in a forthcoming publication.

5 Summary

In this article, we present the first results for the gluon fusion loop-induced sub-process $gg \to ggg\Phi$ at the LHC, where Φ corresponds to a general *CP*-violating Higgs boson. Interference effects between loops with top- and bottom-quarks as well as between *CP*-even and *CP*-odd couplings to heavy quarks are fully taken into account.

The stability of the numerical results is guaranteed by a suitable application of Ward identities and quadruple precision, which are adequate even for bottom-quark dominated configurations.

JHEP10(2014)173

Using a model, we present effects of bottom-quark loop contributions which can lead to visible distortions in the differential distributions of some important observables for large values of $\tan\beta$. We also show that the presence of additional radiation does not alter the main characteristics of the azimuthal angle correlations.

Our study emphasizes the limitations of the effective Lagrangian approximation including the form factor corrections, which is often used in literature as a numerically fast alternative for phenomenological studies. At a center of mass energy of $\sqrt{s} = 13\,\text{TeV}$, we show that the effective theory actually yields accurate results within the boundaries of small $\tan\beta$ for Higgs masses up to 300 GeV (with form factors) and small transverse momenta $p_T^{j\text{max}} \lesssim 200\,\text{GeV}$. Beyond this boundary, the effective theory deviates significantly from the predictions obtained from the full theory. We find no restriction in the validity of the invariant mass of the di-jet system of the leading jets (not shown) for small values of $\tan\beta$. The shape of the azimuthal angle distribution is well described by the effective theory. However, increasing values of $\tan\beta$ lead to visible distortions. A detailed description of the full process will be given in a forthcoming publication. This process will be made publicly available as part of the VBFNLO program.

Acknowledgments

We thank Dieter Zeppenfeld for useful discussions during the development of this project and Paramita Dey for valuable comments on the manuscript. This work was partially funded by the Deutsche Forschungsgemeinschaft via the Sonderforschungsbereich/Transregio SFB/TR-9 Computational Particle Physics. MK acknowledges support by the Grid Cluster of the RWTH-Aachen. FC is funded by a Marie Curie fellowship (PIEF-GA-2011-298960) and partially by MINECO (FPA2011-23596) and by LHCPhenonet (PITN-GA-2010-264564).

References

[1] ATLAS collaboration, *Observation of a new particle in the search for the standard model Higgs boson with the ATLAS detector at the LHC*, *Phys. Lett.* **B 716** (2012) 1 [arXiv:1207.7214] [INSPIRE].

[2] CMS collaboration, *Observation of a new boson at a mass of 125 GeV with the CMS experiment at the LHC*, *Phys. Lett.* **B 716** (2012) 30 [arXiv:1207.7235] [INSPIRE].

[3] A. Soni and R.M. Xu, *Probing CP-violation via Higgs decays to four leptons*, *Phys. Rev.* **D 48** (1993) 5259 [hep-ph/9301225] [INSPIRE].

[4] T. Plehn, D.L. Rainwater and D. Zeppenfeld, *Determining the structure of Higgs couplings at the LHC*, *Phys. Rev. Lett.* **88** (2002) 051801 [hep-ph/0105325] [INSPIRE].

[5] S.Y. Choi, D.J. Miller, M.M. Muhlleitner and P.M. Zerwas, *Identifying the Higgs spin and parity in decays to Z pairs*, *Phys. Lett.* **B 553** (2003) 61 [hep-ph/0210077] [INSPIRE].

JHEP10(2014)173

[6] C.P. Buszello, I. Fleck, P. Marquard and J.J. van der Bij, *Prospective analysis of spin- and CP-sensitive variables in $H \to ZZ \to l_1^+ l_1^- l_2^+ l_2^-$ at the LHC*, *Eur. Phys. J.* **C 32** (2004) 209 [hep-ph/0212396] [INSPIRE].

[7] A. Djouadi, *The anatomy of electro-weak symmetry breaking. I: The Higgs boson in the standard model*, *Phys. Rept.* **457** (2008) 1 [hep-ph/0503172] [INSPIRE].

[8] A. Djouadi, *The anatomy of electro-weak symmetry breaking. II: The Higgs bosons in the minimal supersymmetric model*, *Phys. Rept.* **459** (2008) 1 [hep-ph/0503173] [INSPIRE].

[9] R.M. Godbole, D.J. Miller and M.M. Muhlleitner, *Aspects of CP-violation in the H ZZ coupling at the LHC*, *JHEP* **12** (2007) 031 [arXiv:0708.0458] [INSPIRE].

[10] B.E. Cox, J.R. Forshaw and A.D. Pilkington, *Extracting Higgs boson couplings using a jet veto*, *Phys. Lett.* **B 696** (2011) 87 [arXiv:1006.0986] [INSPIRE].

[11] C. Englert, M. Spannowsky and M. Takeuchi, *Measuring Higgs CP and couplings with hadronic event shapes*, *JHEP* **06** (2012) 108 [arXiv:1203.5788] [INSPIRE].

[12] B. Coleppa, K. Kumar and H.E. Logan, *Can the 126 GeV boson be a pseudoscalar?*, *Phys. Rev.* **D 86** (2012) 075022 [arXiv:1208.2692] [INSPIRE].

[13] S.Y. Choi, M.M. Muhlleitner and P.M. Zerwas, *Theoretical basis of Higgs-spin analysis in $H \to \gamma\gamma$ and $Z\gamma$ decays*, *Phys. Lett.* **B 718** (2013) 1031 [arXiv:1209.5268] [INSPIRE].

[14] A. Freitas and P. Schwaller, *Higgs CP properties from early LHC data*, *Phys. Rev.* **D 87** (2013) 055014 [arXiv:1211.1980] [INSPIRE].

[15] A. Djouadi and G. Moreau, *The couplings of the Higgs boson and its CP properties from fits of the signal strengths and their ratios at the $7+8$ TeV LHC*, *Eur. Phys. J.* **C 73** (2013) 2512 [arXiv:1303.6591] [INSPIRE].

[16] W.-F. Chang, W.-P. Pan and F. Xu, *Effective gauge-Higgs operators analysis of new physics associated with the Higgs boson*, *Phys. Rev.* **D 88** (2013) 033004 [arXiv:1303.7035] [INSPIRE].

[17] J. Shu and Y. Zhang, *Impact of a CP-violating Higgs sector: from LHC to baryogenesis*, *Phys. Rev. Lett.* **111** (2013) 091801 [arXiv:1304.0773] [INSPIRE].

[18] R.V. Harlander and T. Neumann, *Probing the nature of the Higgs-gluon coupling*, *Phys. Rev.* **D 88** (2013) 074015 [arXiv:1308.2225] [INSPIRE].

[19] S. Dawson et al., *Higgs Working Group report of the Snowmass 2013 community planning study*, arXiv:1310.8361 [INSPIRE].

[20] CMS collaboration, *Study of the mass and spin-parity of the Higgs boson candidate via its decays to Z boson pairs*, *Phys. Rev. Lett.* **110** (2013) 081803 [arXiv:1212.6639] [INSPIRE].

[21] CMS collaboration, *Updated results on the new boson discovered in the search for the standard model Higgs boson in the ZZ to 4 leptons channel in pp collisions at $\sqrt{s} = 7$ and 8 TeV*, CMS-PAS-HIG-12-041 (2012).

[22] CMS collaboration, *Evidence for a particle decaying to W^+W^- in the fully leptonic final state in a standard model Higgs boson search in pp collisions at the LHC*, CMS-PAS-HIG-12-042 (2012).

[23] ATLAS collaboration, *Evidence for the spin-0 nature of the Higgs boson using ATLAS data*, *Phys. Lett.* **B 726** (2013) 120 [arXiv:1307.1432] [INSPIRE].

JHEP10(2014)173

[24] CMS collaboration, *Measurement of the properties of a Higgs boson in the four-lepton final state*, *Phys. Rev.* **D 89** (2014) 092007 [arXiv:1312.5353] [INSPIRE].

[25] CMS collaboration, *Measurement of Higgs boson production and properties in the WW decay channel with leptonic final states*, *JHEP* **01** (2014) 096 [arXiv:1312.1129] [INSPIRE].

[26] CMS collaboration, *Properties of the Higgs-like boson in the decay $H \to ZZ \to 4\ell$ in pp collisions at $\sqrt{s} = 7$ and 8 TeV*, CMS-PAS-HIG-13-002 (2013).

[27] V. Del Duca, W. Kilgore, C. Oleari, C. Schmidt and D. Zeppenfeld, *Higgs + 2 jets via gluon fusion*, *Phys. Rev. Lett.* **87** (2001) 122001 [hep-ph/0105129] [INSPIRE].

[28] K. Odagiri, *On azimuthal spin correlations in Higgs plus jet events at LHC*, *JHEP* **03** (2003) 009 [hep-ph/0212215] [INSPIRE].

[29] V. Hankele, G. Klamke, D. Zeppenfeld and T. Figy, *Anomalous Higgs boson couplings in vector boson fusion at the CERN LHC*, *Phys. Rev.* **D 74** (2006) 095001 [hep-ph/0609075] [INSPIRE].

[30] G. Klamke and D. Zeppenfeld, *Higgs plus two jet production via gluon fusion as a signal at the CERN LHC*, *JHEP* **04** (2007) 052 [hep-ph/0703202] [INSPIRE].

[31] K. Hagiwara, Q. Li and K. Mawatari, *Jet angular correlation in vector-boson fusion processes at hadron colliders*, *JHEP* **07** (2009) 101 [arXiv:0905.4314] [INSPIRE].

[32] F. Campanario, M. Kubocz and D. Zeppenfeld, *Gluon-fusion contributions to Φ + 2 jet production*, *Phys. Rev.* **D 84** (2011) 095025 [arXiv:1011.3819] [INSPIRE].

[33] V. Del Duca et al., *Monte Carlo studies of the jet activity in Higgs + 2 jet events*, *JHEP* **10** (2006) 016 [hep-ph/0608158] [INSPIRE].

[34] V. Del Duca, *Higgs production in association with two jets at the LHC*, *Acta Phys. Polon.* **B 39** (2008) 1549 [INSPIRE].

[35] J.R. Andersen, K. Arnold and D. Zeppenfeld, *Azimuthal angle correlations for Higgs boson plus multi-jet events*, *JHEP* **06** (2010) 091 [arXiv:1001.3822] [INSPIRE].

[36] J.M. Campbell, R.K. Ellis and G. Zanderighi, *Next-to-leading order Higgs + 2 jet production via gluon fusion*, *JHEP* **10** (2006) 028 [hep-ph/0608194] [INSPIRE].

[37] H. van Deurzen et al., *NLO QCD corrections to the production of Higgs plus two jets at the LHC*, *Phys. Lett.* **B 721** (2013) 74 [arXiv:1301.0493] [INSPIRE].

[38] F. Campanario and M. Kubocz, *Higgs boson production in association with three jets via gluon fusion at the LHC: gluonic contributions*, *Phys. Rev.* **D 88** (2013) 054021 [arXiv:1306.1830] [INSPIRE].

[39] G. Cullen et al., *Next-to-leading-order QCD corrections to Higgs boson production plus three jets in gluon fusion*, *Phys. Rev. Lett.* **111** (2013) 131801 [arXiv:1307.4737] [INSPIRE].

[40] R.P. Kauffman, S.V. Desai and D. Risal, *Production of a Higgs boson plus two jets in hadronic collisions*, *Phys. Rev.* **D 55** (1997) 4005 [*Erratum ibid.* **D 58** (1998) 119901] [hep-ph/9610541] [INSPIRE].

[41] R.P. Kauffman and S.V. Desai, *Production of a Higgs pseudoscalar plus two jets in hadronic collisions*, *Phys. Rev.* **D 59** (1999) 057504 [hep-ph/9808286] [INSPIRE].

[42] M. Spira, *QCD effects in Higgs physics*, *Fortschr. Phys.* **46** (1998) 203 [hep-ph/9705337] [INSPIRE].

JHEP10(2014)173

[43] K. Arnold et al., *VBFNLO: a parton level Monte Carlo for processes with electroweak bosons*, *Comput. Phys. Commun.* **180** (2009) 1661 [arXiv:0811.4559] [INSPIRE].

[44] K. Arnold et al., *VBFNLO: a parton level Monte Carlo for processes with electroweak bosons — manual for version 2.5.0*, arXiv:1107.4038 [INSPIRE].

[45] K. Arnold et al., *Release note — VBFNLO-2.6.0*, arXiv:1207.4975 [INSPIRE].

[46] K. Hagiwara and D. Zeppenfeld, *Helicity amplitudes for heavy lepton production in e^+e^- annihilation*, *Nucl. Phys.* **B 274** (1986) 1 [INSPIRE].

[47] K. Hagiwara and D. Zeppenfeld, *Amplitudes for multiparton processes involving a current at e^+e^-, $e^\pm p$ and hadron colliders*, *Nucl. Phys.* **B 313** (1989) 560 [INSPIRE].

[48] M.S. Chanowitz, M. Furman and I. Hinchliffe, *The axial current in dimensional regularization*, *Nucl. Phys.* **B 159** (1979) 225 [INSPIRE].

[49] F. Campanario, *Towards $pp \to VVjj$ at NLO QCD: bosonic contributions to triple vector boson production plus jet*, *JHEP* **10** (2011) 070 [arXiv:1105.0920] [INSPIRE].

[50] G. Passarino and M.J.G. Veltman, *One loop corrections for e^+e^- annihilation into $\mu^+\mu^-$ in the Weinberg model*, *Nucl. Phys.* **B 160** (1979) 151 [INSPIRE].

[51] A. Denner and S. Dittmaier, *Reduction schemes for one-loop tensor integrals*, *Nucl. Phys.* **B 734** (2006) 62 [hep-ph/0509141] [INSPIRE].

[52] G. 't Hooft and M.J.G. Veltman, *Scalar one loop integrals*, *Nucl. Phys.* **B 153** (1979) 365 [INSPIRE].

[53] A. Denner, U. Nierste and R. Scharf, *A compact expression for the scalar one loop four point function*, *Nucl. Phys.* **B 367** (1991) 637 [INSPIRE].

[54] J. Alwall et al., *MadGraph/MadEvent v4: the new web generation*, *JHEP* **09** (2007) 028 [arXiv:0706.2334] [INSPIRE].

[55] J. Alwall, M. Herquet, F. Maltoni, O. Mattelaer and T. Stelzer, *MadGraph 5: going beyond*, *JHEP* **06** (2011) 128 [arXiv:1106.0522] [INSPIRE].

[56] F. Campanario, Q. Li, M. Rauch and M. Spira, *ZZ + jet production via gluon fusion at the LHC*, *JHEP* **06** (2013) 069 [arXiv:1211.5429] [INSPIRE].

[57] J. Pumplin et al., *New generation of parton distributions with uncertainties from global QCD analysis*, *JHEP* **07** (2002) 012 [hep-ph/0201195] [INSPIRE].

[58] J.A.M. Vermaseren, S.A. Larin and T. van Ritbergen, *The four loop quark mass anomalous dimension and the invariant quark mass*, *Phys. Lett.* **B 405** (1997) 327 [hep-ph/9703284] [INSPIRE].

[59] F. Campanario, T.M. Figy, S. Plätzer and M. Sjödahl, *Electroweak Higgs boson plus three jet production at next-to-leading-order QCD*, *Phys. Rev. Lett.* **111** (2013) 211802 [arXiv:1308.2932] [INSPIRE].

JHEP10(2014)173